WAVE RESPONSE OF CLOSED FLEXIBLE BAGS

Pål Lader
SINTEF Ocean
7465 Trondheim, Norway
pal.lader@sintef.no

David W. Fredriksson
United States Naval Academy
Annapolis, MD 21402, USA
fredriks@usna.edu

Zsolt Volent
SINTEF Ocean
7465 Trondheim, Norway
zsolt.volent@sintef.no

Jud DeCew
University of New Hampshire
Durham, NH 03824, USA
jdecew@gmail.com

Trond Rosten
SINTEF Ocean
7465 Trondheim, Norway
trond.rosten@sintef.no

Ida M. Strand
Norwegian University of Science and Technology
7491 Trondheim, Norway
ida.strand@ntnu.no

ABSTRACT

Recent environmental considerations, as salmon lice, escape of farmed fish and release of nutrients, have prompted the aquaculture industry to consider the use of closed fish production systems. The use of such systems is considered as one potential way of expanding the salmon production in Norway.

To better understand the response in waves of such bags, experiments were conducted with a series of 1:30 scaled models of closed flexible bags. The bags and floater were moored in a wave tank and subjected to series of regular waves (wave period between 0.5 and 1.5s and wave

steepness 1/15, 1/30 and 1/60). Three different geometries were investigated; cylindrical, spherical and elliptical, and the models was both tested deflated (70% filling level) and inflated (100% filling level). Incident waves were measured together with the horizontal and vertical motion of the floater in two points (front and aft). Visual observations of the response were also done using cameras.

The main finding from the experiments were that a deflated bag was more wave compliant than an inflated bag, and that the integrity (whether water entered or left the bag over the floater) was challenged for the inflated bags even for smaller waves (identified as wave condition B (1.0m<H<1.9m) in Norwegian Standard NS 9415). A deflated bag is significantly more seaworthy than an inflated bag when it comes to integrity and motion of the floater.

INTRODUCTION

Recent environmental considerations, as salmon lice, escape of farmed fish and release of nutrients, have prompted the Norwegian aquaculture industry to consider the use of closed fish production systems (CFPS). The use of such systems is amongst other suggestions also considered as a potential way of expanding the salmon production in Norway [1]. In a closed system, the farmer can target increased control of how the fish are exposed to pathogens, parasites, algaes or pollution, by controlling the flow and quality of water going in and out of the containment volume. This may establish a more bio-secure production environment, and the use of these systems can contribute to changes in production regimes, e.g. larger smolts and a shorter on-growing phase in sea.

Internationally the aquaculture industry has broadly considered three types of CFPS; 1) land based flow through or recirculation systems, 2) floating systems with rigid containment and 3) floating systems with flexible containment (See e.g. [2]). The concept of floating closed flexible cages (CFC) (3) offers a route for developing CFPSs that might be faster than developing new CFPS with rigid material (1 & 2). The rationale behind this is that flexible floating systems are

not far from the conventional net-based fish farm systems, and can be used in existing floating fish farms (both circular plastic and square steel farms) in combinations with net cages. Even though there is a strategic argument for the light and strong flexible floating system, numerous research challenges exist.

There are few examples where closed flexible membranes are used in design of ocean structures. The structure that mostly resembles a closed flexible fish cage is the "water bag", of which the first reported application was the *Dracone barge* [3]. This is a concept for transporting or storing large quantities of fresh water or other liquid lighter than the surrounding water. Such water bags have been subjected to both numerical and experimental studies of the behavior in waves ([4], [5], [6] and [7]). The closed flexible cage adds, however, to the complexity by having an internal volume of water that has a free surface and an internal flow that is of significant importance to the whole problem.

Different from a net based cage, the bag represents a closed volume of water and in dynamic situations, such as in waves; the accelerated mass of the bag structure also includes the water inside the bag. This makes the closed bag a large volume structure, and it will behave differently in waves compared to a conventional net based structure which must be considered to be a small volume structure.

Similar to a flexible net based cage, the flexibility and deformation of the bag is closely coupled to the hydrodynamic forces, making the hydrodynamic load more complex than for a rigid structure. Net based gravity cages are also very compliant and it is well known that attachment and mooring loads can be reduced due to the deflection of the net. The deformation characteristics of a closed bag will however be dependent upon the internal water level, more specifically; if the bag is inflated or not. A deflated bag allows more deformation than an inflated bag. The inflated state is the normal mode of operation, but a deflated state may come as a consequence of damage or certain operational considerations.

In this work the response in regular waves of such bags was studied, and the dependency on the filling level especially addressed. This work is part of a larger project on closed flexible cages and other results have been previously reported [8-10] .

EXPERIMENTAL SETUP AND PROCEDURE

In this work, the behavior of closed flexible bags in regular waves was investigated through scaled model experiments in a small wave tank. As mentioned in the introduction the motivation for studying these structures is their use as fish farms with the possibility to totally control water quality inside the bag. A fish farm consists of a floater, a cage and a mooring system. The floater can have different shape, the most used forms are circular, and from the floater the cage is hung so that it encloses a water volume. The cage is usually made of net, allowing the water to flow freely in and out of the cage, but here the cage (or *bag* as it can be described when it is closed) is made of fabric that is not permeable. The geometry of the bag can have different shapes, and in order to get an overview of the behavior of the most relevant geometries, three different bag shapes were studied: Cylindrical, spherical and elliptical (Figure 1).

Bag models

Presently there exist few examples of full scale versions of fish cages with closed flexible bags, and therefore there is no industry standard for how to construct these bags. The models were thus made as generic as possible.

The models all had a floater circumference of 764 mm and were assumed to have a scale of 1:30. The corresponding full scale structures would have a diameter of 22.9 m (circumference = 72 m), and a volume between 3000 and 5000 m^3. Although considerably smaller than the industry standard for conventional cages, this size is representative for some of the present experimental initiatives on closed cages (e.g. the MSC Aqua AS's "Aquadome").

Based on the tarpaulin material used in some of few closed flexible cages build, it was decided to assume neglectable bending stiffness in the bag. Based on this it was chosen to use

the same type of woven nylon material as used in parachutes. This textile was 0.04 mm thick, and weighted 40 g/m^2. It is considered water proof, and the bags were constructed by sewing together the difference sheets using wool tread. Wool expands in water and increases the water proofing of the seams. The intention was that the amount of water in the bag should be constant during the experiments, and this was achieved to a high degree.

For a conventional net based cage a weight system is necessary to maintain shape and volume. For a closed bag however, the weight system will play a much different role than on a net based cage since the volume is constant. The effect of the weight system may only come into play when the bag is not inflated. It is uncertain what kind of weight system that will be used on industrial size closed flexible bags in the future, if any. It was therefore decided not to have any weights attached to the model.

Floater model

The floater model was made of PVC tubing used for electrical cable conduit. The dimensions and stiffness properties are given in Table 1. A single pipe was used in the model, although for an industrial scale farm two (or three) pipes are usually used to construct the floater. As can be seen from the table, the floater volume and the stiffness around the horizontal axis (EI_x) is well modelled, but the stiffness around the vertical axis (EI_z) is too low in the model. This was not considered to be critical, since the horizontal shape is maintained by the mooring lines.

Filling levels

The most likely mode of operation for such a closed bag system is for the bag to be slightly overfilled (inflated) causing the pressure inside the bag to be larger than on the outside. This pressure difference helps to maintain the overall shape of the bag, as an inflated bag can only deform if 1) the bag materials flexibility allow in-plane axial deformation, and/or 2) the free surface water level inside the bag rises. When the bag is exposed to current there will be some local deformation due to the flexibility of the material, but the overall shape will be kept due to

the enclosed water volume. If the bag is deflated however, the bag will be allowed to globally deform. A lower filling level, and consequently deflation of the bag, could be caused by damage to the bag for example, or it can be necessary due to operational considerations. It was thus interesting to also study how the bags would behave when they have a lower filling level, since it could be assumed that this would significantly influence the behavior. In previous work, large differences between inflated and deflated states have also been found [8-10]. Both an inflated (100%+ filling level) and a deflated (70% filing level) state were therefore used in the experiments. The filling level is given as percentage of the theoretical volume calculated from the main dimensions as given in Figure 1. In the inflated state (100%+) the bag is filled until the floater is half way submerged, which means a filling level slightly more than the theoretical volume (from 3% to 8% more than the theoretical volume depending on the geometry), thus the "+" sign in the filing level label (100%+).

Tank facilities

The experiments were conducted at the Hydromechanics laboratory at the United States Naval Academy in Annapolis, Maryland, USA in August 2012. The towing tank used in the experiments was 2.45 meter wide, 1.52 meter deep and 36 meter long (Figure 2).

Setup

The general layout of the tank with the model is shown in Figure 3 and Figure 4. The model is moored using four lines. The front and back moorings are attached to a spring and a load cell. The stiffness of the springs are chosen to be in a range characteristic for a conventional system mooring setup (k = 10.5 N/m). The side moorings are attached to a counter weight of 1.5 N, and the front/back mooring is pretensioned equally. The load cells allow measuring of the horizontal displacement of the front and back point of the floater. To measure the vertical displacement of these points, two vertical lines are attached and led up to a spring and a load cell (see also Figure 3). The spring stiffness of this spring is chosen so that the force contribution from this line to the floater can be neglected (k = 0.67 N/m). The force acting on the floater

from this line would be less than 1.5% of the floaters displaced mass. In this setup, the horizontal motion of the floater introduces an error in the measurements of the vertical position since the line between the measurement point and the load cell will have a small time varying angle. This error can be minimized by maximizing the vertical distance between the measurement point and the load cell. In this setup, this length was more than 3 meters. With a maximum horizontal displacement of approximately 10 cm this limits the error to less than 0.2%. Two capacitance wave gauges were also used in the setup and positioned as shown in Figure 4. All waves were run without the presence of the model in order to measure the undisturbed incidence wave height. The measurements were logged with 50 Hz, and each run had duration of 90 seconds. In addition to measuring the waves and the motion response of the model, three cameras were used to record the motion and deformation of the bag fabric. The deformation was only recorded qualitatively, and no quantitative data was derived from the images. The cameras were placed behind, in front, on the side, and under the model.

Wave cases

The bag models were subjected to regular waves with varying period and steepness. The wave period was varied between 0.5s to 1.5s in 0.1s increments, and for each period, three different wave steepnesses (1/60, 1/30 and 1/15) were used, resulting in a total of 33 different regular wave cases as shown in Table 2. The wave length of these waves corresponded to 0.5 to 4.6 times the cage diameter. Full scale values of wave period and height are also given in the table (assuming the models had a 1:30 scale), and the full scale wave heights runs from 0.2 to 7.0 m. The wave classification according to the industry standard NS9415:2009 is shown in the table.

Experimental matrix

In Figure 5 the combinations of bag geometry, filling levels and waves are shown. Due to time and practical limitations it was not possible to perform all the possible combinations,

therefore it was chosen to focus on Subset 1) 1/30 wave steepness and Subset 2) the inflated spherical bag. The following analysis is based mainly on these two subsets.

RESULTS AND DISCUSSION

Integrity of the bag

One of the objectives of the model experiments was to investigate the integrity of the bag, i.e. if there is water exchange between the internal volume of the bag, and the surrounding water. The main motivation for a closed cage concept is to have control of the water in the system to avoid chemical or biological contamination. Needless to say, the bag needs to maintain its integrity in order to achieve this. The integrity can be compromised in different ways, like a hole in the bag fabric, but in this study it is the water exchange over the floater rim due to the relative motion between the rim and the free surface that is examined. In each run, the exchange of water over the rim was visually identified, and the results are shown in Figure 6. Clearly the deflated state (70% filling) is favourable with respect to integrity. As shall also be seen later, this is caused by the difference in motion response of the floater, which in turn is dependent on the coupling between the response of water contained in bag and the floater. In the deflated state, the response of the mass of the water enclosed in the bag is more decoupled from the floater motion, since the bag is allowed to deform. This allows the floater to follow the water surface, maintaining the integrity of the bag. In the inflated state, the floater is forced to follow the motion of the enclosed water, and this influences the relative motion between the floater and the water surface such that the water overflowed the floater exchanging water between the inside and the outside.

As can be seen from the results, for the inflated state, which is the most probable operational state, the integrity is challenged even for the class A waves when the waves are steep (s=1/15), but for lower steepness (1/30) integrity is maintained for class A, and for 1/60 even for class B.

This means that the inflated bag is not very wave compliant, and that the bag in this state can only be operated in very limited wave conditions if the integrity of the bag is important.

All the three different geometries show the same behaviour for wave steepness 1/30, but for the steepest waves (1/15) the integrity characteristics are different. This indicates that the choice of geometry might be important in energetic wave situations and this needs to be further investigated.

Wave response of the floater

The wave response of the floater is investigated by measuring the horizontal and vertical motion of two points; one in the front and one in the back of the floater, and analyzing this together with wave measurements of undisturbed waves (see Figure 3 and Figure 4). The analysis of the wave response presented in this paper is limited to the first harmonic component, with and the higher order components neglected. This does not mean that higher order components are insignificant, and the motion of the bag certainly contains significant higher order components that should be analyzed. However, higher order components were omitted in order to limit the scope of the paper. Four different response modes are analysed; heave front, heave back, surge global and a horizontal flexible mode. The heave response is the vertical motion of each of the two points on the rim of the floater, while the global surge is the mean horizontal position, and the flexible mode is the difference between the horizontal positions (subtracted the cage diameter) of the two points. From each of these modes the response amplitude operator (RAO) is calculated as the square root of the ratio between the energy in the response mode and the energy in the wave. The energy is calculated from the power spectral density (PSD) by integrating the PSD in the frequency area $f=[0.9\ f_{1stharmonic}\ ,\ 1.1\ f_{1stharmonic}]$, thus isolating the energy in the first harmonic peak. The RAO as a function of wave length are shown in Figure 7 (for the cases with wave steepness 1/30, dotted area in Figure 5) and Figure

8 (for the spherical bag, dashed area in Figure 5). The wave length is calculated from the wave frequency using deep water assumption, and then normalized with respect to cage diameter.

Considering first the heave response for the different tarpaulin shapes and filling levels (the cases with constant wave steepness H/L=1/30, top two plots in Figure 7) it is clear that the observations that was done earlier with respect to integrity is reflected in the heave response. When the bags are deflated, the floater follows the wave since the floater is decoupled from the motion of the bag, and the response of the floater is almost independent on the bag geometry. For the inflated states however, the bag geometry is significantly influencing the heave response of the floater forcing the floater to have a smaller response, and thus compromising the integrity of the bag as the waves overtops the floater rim. The difference in response for the different bag shapes is coupled to the depth of the bag. The vertical component of the wave excitation force, that drives the vertical response, is the dynamic pressure times the vertical component of the surface normal vector integrated over the wet surface. Needless to say, this force is larger when the surface with vertical normal components is higher up in the wave zone, and thus the spherical bag will have the largest vertical wave excitation force, and the cylindrical bag will have the smallest, in accordance with the response RAO for the bags.

The surge responses have a clear extinction point at $L/D \approx 1.7$ for all the inflated cases, and this is because the force on the front and rear side of the bags cancel each other out at this wave length. This corresponds well with observations for flexible net cases [11]. For the deflated states, the extinction is not as clearly defined, and comes at a shorter wavelength ($L/D \approx 1.4$). The cause of this is the same as have been described earlier, that the motion of the bag is somewhat decoupled from the floater motion when the bag is deflated. The elliptical bag show a significant different behavior from the others in the deflated case (70%), but it is difficult to find a good explanation for this since this distinct difference only occur in the surge response, and it cannot be ruled out if this is due measurements errors.

The response in the flexible mode shows the same difference between the inflated and the deflated cases as seen in the other response modes. Significantly more energy is transferred to the flexible mode for inflated cases compared to the deflated. This is again due to the decoupling of the bag from the floater in the deflated cases. It is also worth noticing that the energy in the flexible mode is larger than the global surge for lower wave lengths (below approximately L/D=3), but as the wavelength increases the energy in the surge mode becomes the most energetic. This is natural since the surge is driven by the sum of the forces on the front and the rear side of the bag, and the flexible mode is driven by the difference of the front and rear force.

In linear theory the RAO should be independent of the wave steepness, and in Figure 8 the RAOs for the inflated spherical bag is shown for waves with different steepnesses. From this it can be seen that the flexible mode have a highly non-linear characteristic since it is clearly dependent on the wave steepness. The surge response RAO, on the other hand, have a weaker dependency on wave steepness, the same is the case for the heave response. This highly nonlinear behavior is probably due to the coupling with the oscillation of the internal water volume and sloshing waves. This emphasizes the complex behavior of these structures, and the strong coupling between the dynamics of the internal water and the response of the whole structure.

Wave drift force

The wave response in surge have two main components, the first order response (as just discussed), and the mean displacement. The mean displacement is caused by the mean wave drift force (WDF), and this force represents the force that the mooring system needs to be dimensioned to withstand. It is thus an important feature of such a structure. The WDF is calculated directly from the time averaged vertical displacement of the cage and the spring constant, and is shown in Figure 9. Again, the difference between the inflated and deflated cases is significant, and is caused by the deflated cases ability to deform. This deformation dampens

the incoming wave energy and causes less of this energy to be converted to drift force acting on the bag. The deflated cases lower WDF adds to the positive features deflated states show in waves; it has earlier been shown that the integrity of the cage is better maintained if the bag is deflated. Considering the inflated states, the WDF for all the three geometries are overlapping and this indicates that the WDF is more or less independent of the bag geometry, but dependent on the bag volume (keep in mind that the WDF is normalized with respect to the bag volume in the plots). It can also be seen that the wave drift force is highly dependent on the wave steepness. This comes as no surprise, since the WDF must be assumed to be proportional to the wave height squared.

Bag fabric motion

Even though the motion of the bag fabric is not within the scope of this paper is relevant to make a few comments regarding this. The fabric motion was not measured, but could be observed from the cameras that were used. The fabric showed a fluttering behavior in both the inflated and deflated cases, but apparently more energetic in the inflated cases. Even though it is not confirmed with measurements, it is possible that this fluttering motion could introduce snap loads in the bag. This needs to be investigated further with quantitative measurements of the flutter phenomenon.

CONCLUSIONS

Based on the measurements and observations of the floater motion in waves it is clear that a closed flexible cage has large challenges in waves. For an inflated state, the normal mode of operation, the bags integrity is maintained only for waves with a wave height less than 1 m (corresponding to the lowest wave class in NS 9415, Wave class A) for wave steepness 1/30. This was similar for all the three different bag geometries, but the elliptical bag showed better integrity characteristics in steeper waves (1/15) than the two others. When the bag was deflated however, the wave response of the floater was different, and the integrity of the bag was

maintained at more energetic waves than for the inflated case. The RAO of the floater response also showed this, and the behaviour in waves seemed to improve when the bag was deflated.

It must be emphasized that the findings in this work is based on measurements of the floater motion only and only visual observations of the motion of the bag itself. The motion of the floater, and the integrity of the bag indicate that a deflated bag behaves significantly better in waves than an inflated bag. It is however important to take the motion and deformation of the bag into account before any conclusions about this is made. The visual observations of the deflated bag during wave exposure show that the bag behaves rather violently, and it can be assumed that snap loads in the bag fabric may occur. The interaction and coupling between the internal body of water, the bag and floater, and the external water is complex, and have significant nonlinear characteristics as can be seen from the RAO of the flexible modes of the floater. This needs to be further investigated in order to improve the seaworthiness of these structures.

ACKNOWLEDGEMENT

Funding was provided by the Norwegian Research Council's 'Havbruk' programme to the project External Sea Loads and Internal Hydraulics of Closed Flexible Cages (CFC) (grant no. 216127). The authors would like to thank the professional and technical staff at the U.S. Naval Academy Hydromechanics Laboratory for their support. The work conducted by the United States Naval Academy was done through a CRADA agreement with the University of New Hampshire which had a subcontract with SINTEF.

REFERENCES

[1] Gullestad, P., Bjørgo, S., Eithun, I., Ervik, A., Gudding, R., Hansen, H., Johansen, R., Osland, A. B., Rødseth, M., Røsvik, I. O., Sandersen, H. T., and Skarra, H., 2011, "Effektiv og bærekraftig arealbruk i havbruksnæringen (in Norwegian)," Rapport fra et ekspertutvalg

oppnevnt av Fiskeri- og kystdepartementet, The Royal Norwegian Ministry of Fisheries and Coastal Affairs, Oslo, Norway.

[2] Chadwick, E. M. P., Parsons, G. J., and Sayavong, B., eds., 2010, *Evaluation of closed-containment technologies for saltwater salmon aquaculture*, NRC Research Press, Ottawa, Chapter 5, pp. 57-110.

[3] Hawthorne, W. R., 1961, "The early development of the dracone flexible barge," Proceedings of the Institution of Mechanical Engineers, **175**(1), pp. 52-83.

[4] Zhao, R., and Aarsnes, J. V., 1998, "Numerical and experimental studies of a floating and liquid-filled membrane structure in waves," Ocean Engineering, **25**(9), pp. 753-765.

[5] Zhao, R., and Triantafyllou, M. S., "Hydroelastic analyses of a long flexible tube in waves," Proc. International Conference on Hydroelasticity in Marine Technology, O. Faltinsen, ed., pp. 287-300.

[6] Das, S., and Cheung, K. F., 2009, "Coupled boundary element and finite element model for fluid-filled membrane in gravity waves," Engineering Analysis with Boundary Elements, **33**(6), pp. 802-814.

[7] Phadke, A. C., and Cheung, K. F., 2003, "Nonlinear response of fluid-filled membrane in gravity waves," Journal of Engineering Mechanics, **129**(7), pp. 739-750.

[8] Lader, P., Fredriksson, D. W., Volent, Z., DeCew, J., Rosten, T., and Strand, I. M., 2015, "Drag Forces on, and Deformation of, Closed Flexible Bags," Journal of Offshore Mechanics and Arctic Engineering, **137**(4), pp. 0412021 - 0412028.

[9] Strand, I. M., Sørensen, A. J., Lader, P. F., and Volent, Z., 2013, "Modelling of Drag Forces on a Closed Flexible Fish Cage," 9th IFAC Conference on Control Applications in Marine Systems, 9(1), pp. 340-345.

[10] Strand, I. M., Sørensen, A. J., and Volent, Z., "Closed Flexible Fish Cages: Modelling and Control of Deformations," Proc. 33rd International Conference on Ocean, Offshore and Arctic Engineering, p. V08AT06A005.

[11] Kristiansen, T., and Faltinsen, O. M., 2015, "Experimental and numerical study of an aquaculture net cage with floater in waves and current," Journal of Fluids and Structures, **54**, pp. 1-26.

LIST OF TABLES

LIST OF FIGURES

mode I. RAO is calculated as the square of the ration between the energy in the response mode and the energy in the wave. The energy is calculated from the power spectral density (PSD) by integrating the PSD in the frequency area $f=[0.9\ f_{1stharmonic}\ ,\ 1.1\ f_{1stharmonic}]$, thus isolating the energy in the first harmonic peak.

Figure 8. 1st harmonic response amplitude operator (RAO) for the spherical bag (dashed area in Figure 5). The calculation of RAO is explained in the caption of Figure 7.

Figure 9. Mean wave drift force. The force is given as a percent of the displace volume (100%+ inflated state) times $\rho\ g$ (water density and the acceleration of gravity). The mean wave drift force is calculated from the mean surge displacement (x-direction) using the spring constant of the mooring lines along the x-axis. The contribution from the mooring along the y-axis to the force in x-direction is neglected. This is justified by the mean displacement in surge being less than 10 cm, and for such a displacement the force contribution from the y-direction mooring lines is less than 10% of the force in the x-direction mooring lines.

TABLES

	Model (scale 1:30)	Full scale conversion	Real farm	
Floater configuration	Single pipe, 'electrical tube'		Double pipe spaced a diameter apart, HDPE	
Floater circumference	2.40	72.0	72.0	[m]
Floater diameter	0.764	22.9	22.9	[m]
Pipe diameter	0.024	0.71	0.50	[m]
SDR (Standars Dimention Ratio)			17	[-]
Floater cross section area	4.34E-04	0.390	0.393	[m^2]
Area of inertia floater pipe(s) cross section, horizontal axis (I_x)			0.0029	[m^4]
Area of inertia floater pipe(s) cross section, vertical axis (I_z)			0.0246	[m^4]
Yongs Modulus (E)			0.8	[Gpa]
EI_x	8.54E-02	2.08E+06	2.31E+06	[Nm^2]
EI_z			1.97E+07	[Nm^2]
Floater volume	1.04E-03	28.11	28.28	[m^3]

Table 1. The floater dimensions and stiffness properties.

Model scale					L/D	Full scale (1:30)				
		Wave steepness						Wave steepness		
		1/60	1/30	1/15				1/60	1/30	1/15
T	L	H			L/D	T	L	H		
[s]	[m]	[cm]			[-]	[s]	[m]	[m]		
0.5	0.39	0.7	1.3	2.6	0.5	2.7	11.7	0.2	0.4	0.8
0.6	0.56	0.9	1.9	3.7	0.7	3.3	16.9	0.3	0.6	1.1
0.7	0.77	1.3	2.6	5.1	1.0	3.8	23.0	0.4	0.8	1.5
0.8	1.00	1.7	3.3	6.7	1.3	4.4	30.0	0.5	1.0	2.0
0.9	1.26	2.1	4.2	8.4	1.7	4.9	37.9	0.6	1.3	2.5
1.0	1.56	2.6	5.2	10.4	2.0	5.5	46.8	0.8	1.6	3.1
1.1	1.89	3.1	6.3	12.6	2.5	6.0	56.7	0.9	1.9	3.8
1.2	2.25	3.7	7.5	15.0	2.9	6.6	67.4	1.1	2.2	4.5
1.3	2.64	4.4	8.8	17.6	3.5	7.1	79.2	1.3	2.6	5.3
1.4	3.06	5.1	10.2	20.4	4.0	7.7	91.8	1.5	3.1	6.1
1.5	3.51	5.9	11.7	23.4	4.6	8.2	105.4	1.8	3.5	7.0

NS9415:2009 Wave clasifications (H=1.9*Hs)	
A	H < 1.0 m
B	1.0 m < H < 1.9 m
C	1.9 m < H < 3.8 m
D	3.8 m < H < 5.7 m
E	5.7 m < H

Table 2. Overview over the regular wave cases used in the experiments. The wave period was varied between 0.5 s and 1.5 s, and for each period three wave steepnesses (s = 1/60, 1/30 and 1/15) were run. In the table the full scale values are also shown (assuming a 1:30 scale). A non-dimensional wavelength (L/D) where the wave length (L) is normalized with respect to the cage diameter (D) is also shown in the table. This parameter will be used in the analysis. The wave length (L) is calculated using the linear dispersion relation for deep water. In the full scale wave heights the wave classification from the industry standard NS9415:2009 is indicated using different grey scale shading. Note that in the standard it is assumed irregular waves and each wave class is defined by an interval in significant wave height (Hs) and peak period (Tp). If regular wave is considered, as it is in this case, the standard says that the corresponding wave height (H) can be assumed to be 1.9 times the significant wave height (Hs). This is used here. The wave period is not taken into consideration and the wave classification should thus only be taken as a crude indication on the severity of the considered regular wave cases.

FIGURES

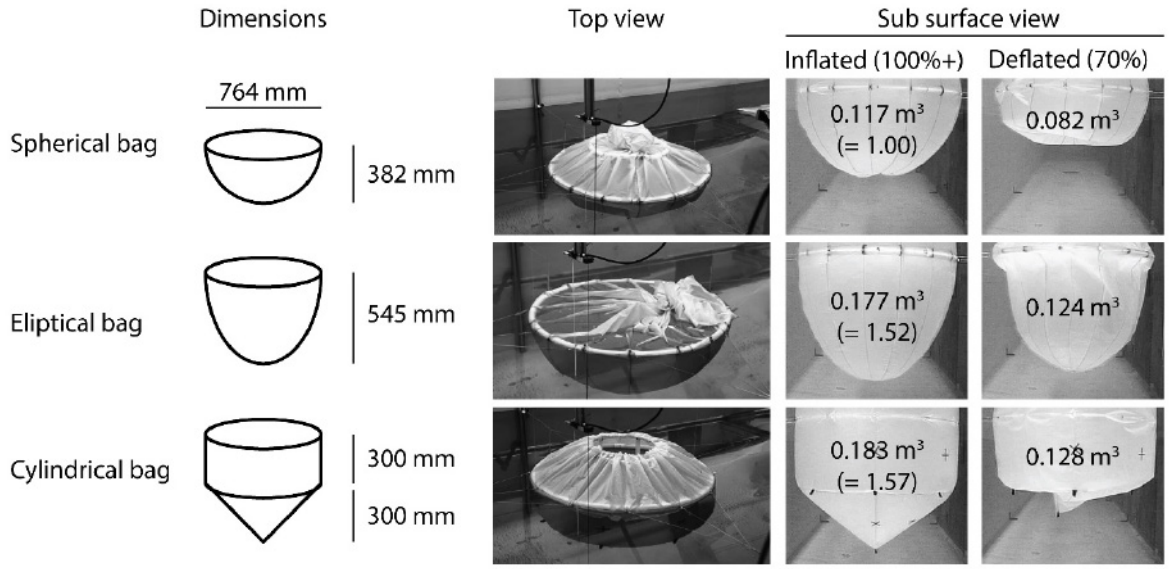

Figure 1. Overview over bag models used in the experiments. Each bag model was tested with both an inflated and a deflated state. The deflated state had a filling level corresponding to 70% of the theoretical bag volume (the theoretical volume is the volume given in the figure), while the inflated state had a filling level slightly more than the theoretical volume (100%+). The floater cross ection is circular with a diameter of 2.4 cm, and for the deflated states the floater is aproximately 10 % submerged, and 50% submerged for the inflated states. This means that the freeboard of the floater is approximately 2.1 cm (deflated states) and 1.2 cm (inflated states). It is assumed that these models are 1:30 representations of full scale bags (In full scale the diameter of the floater is 22.9 m with a circumference of 72 m, and the displace volume for the spherical bag is 3 152 m3). The expansion of the bag fabric over the free surface (as seen on the top view) does not represent a structural part and is purely due to experimental practicalities. By closing of the free surface water is prevented from entering or leaving the volume in the most severe wave cases. This is practical since it is important to have control of the amount of water inside the bag. Even though the fabric in the model experiments maintain the integrity of the model bag it is easily observed when the integrity of the bag would have been challenged if the surface fabric was not present.

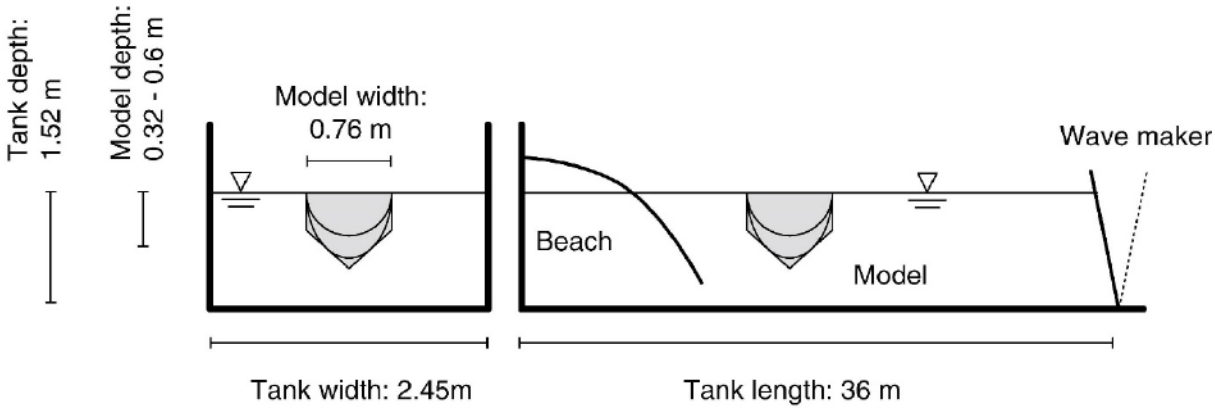

Figure 2. The towing tank facilities at the United States Naval Academy. The tank is equipped with a hinged wave maker and a wave absorbing beach.

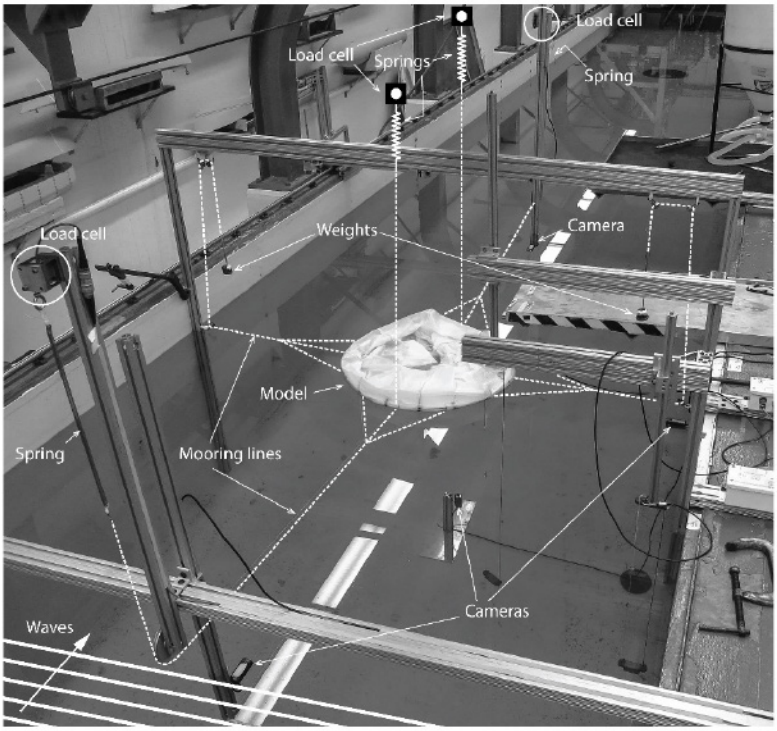

Figure 3. Overview of the experimental setup. A schematic drawing with details is shown in Figure 4.

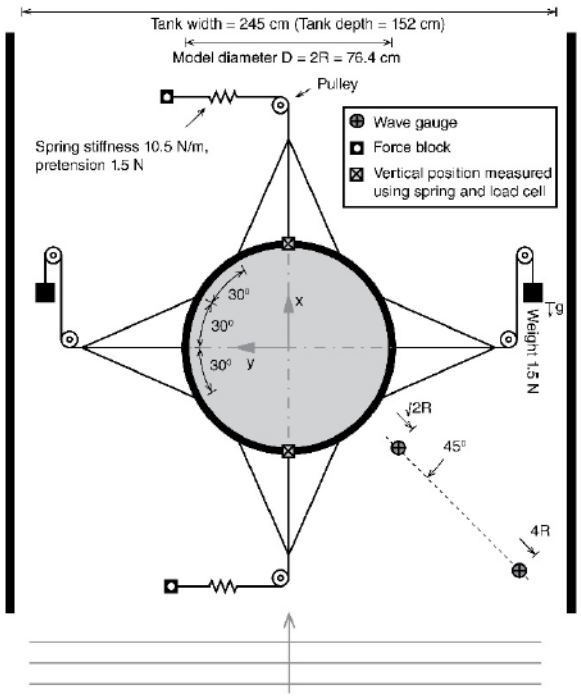

Figure 4. A schematic drawing of the experimental setup.

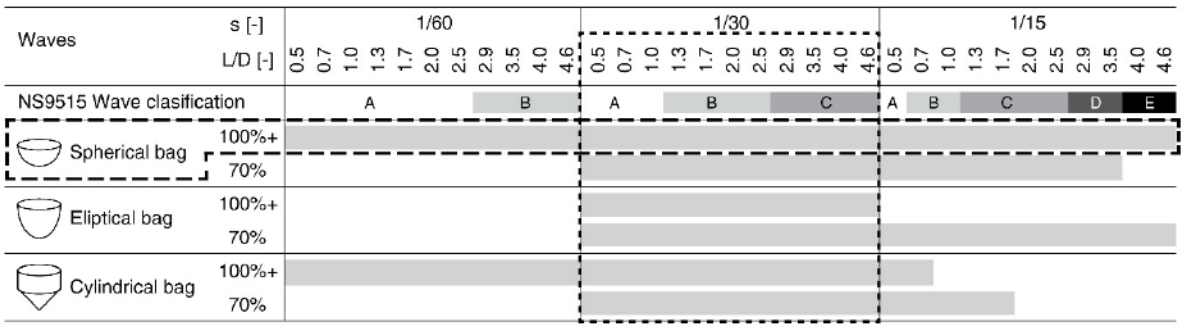

Figure 5. Overview over combinations of models, filling levels and wave cases that were run. The wave cases are identified by wave the non-dimensional parameters wave steepness (s) and wave length normalized with respect to bag diameter (L/D). The areas indicated with the dashed and dotted lines are the model/wave combinations that are used in the analysis of the dynamic response.

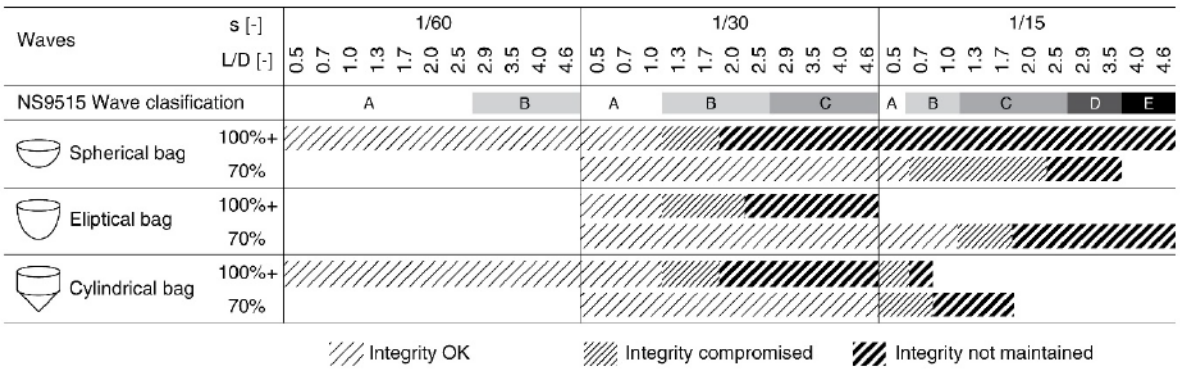

Figure 6. Integrity of the bags at different wave cases. Integrity is understood as the ability to prevent any water exchange between the volume inside the closed bag and the outside water volume. The integrity of the bags in each case was established through visual observations of whether or not water could enter or leave the bag over the rim of the floater.

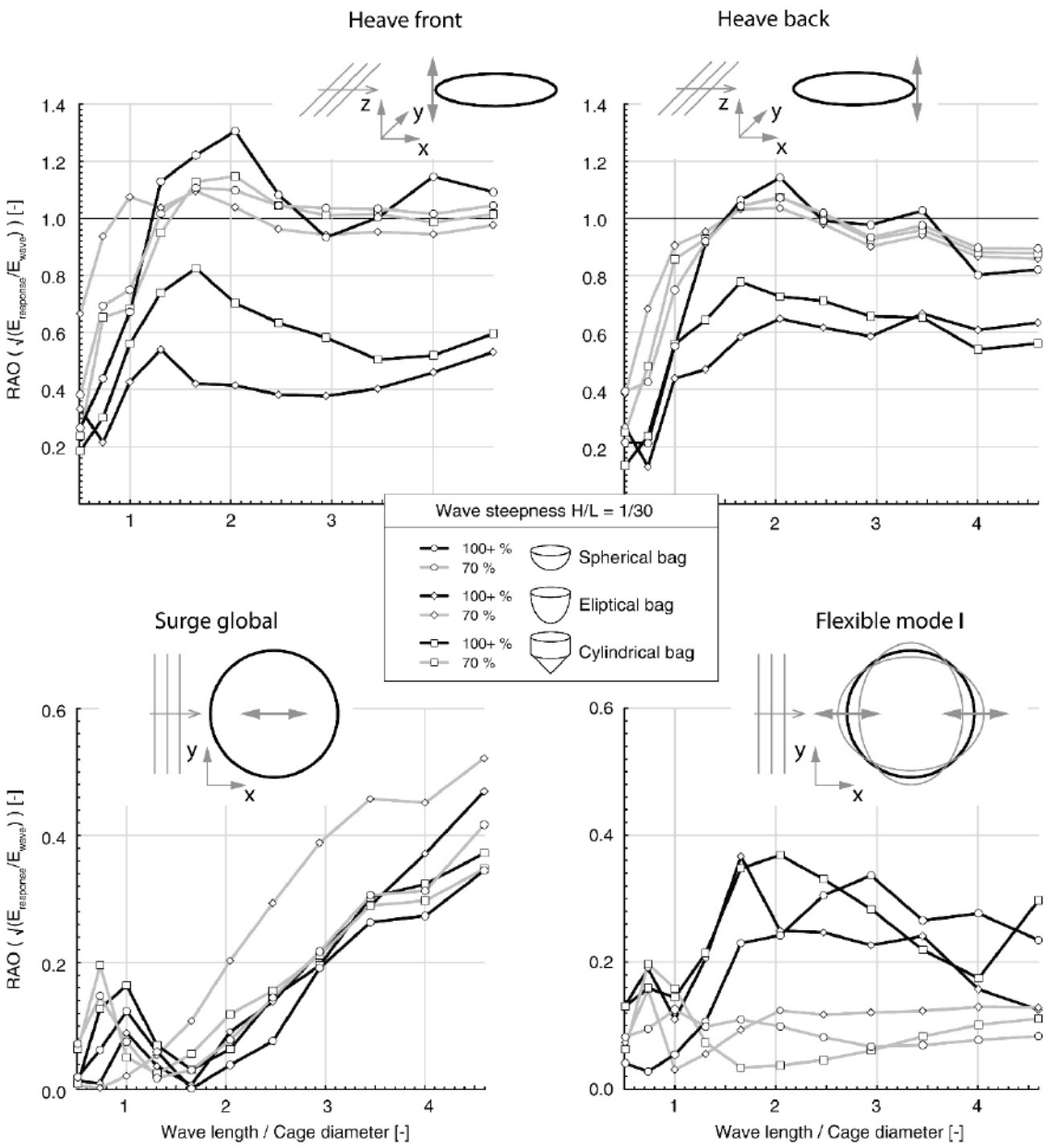

Figure 7. 1st harmonic response amplitude operator (RAO) for the cases with wave steepness 1/30 (dotted area in Figure 5). Four different response modes are shown; heave front, heave back, surge global and flexible mode I. RAO is calculated as the square of the ration between the energy in the response mode and the energy in the wave. The energy is calculated from the power spectral density (PSD) by integrating the PSD in the frequency area f=[0.9 $f_{1stharmonic}$, 1.1 $f_{1stharmonic}$], thus isolating the energy in the first harmonic peak.

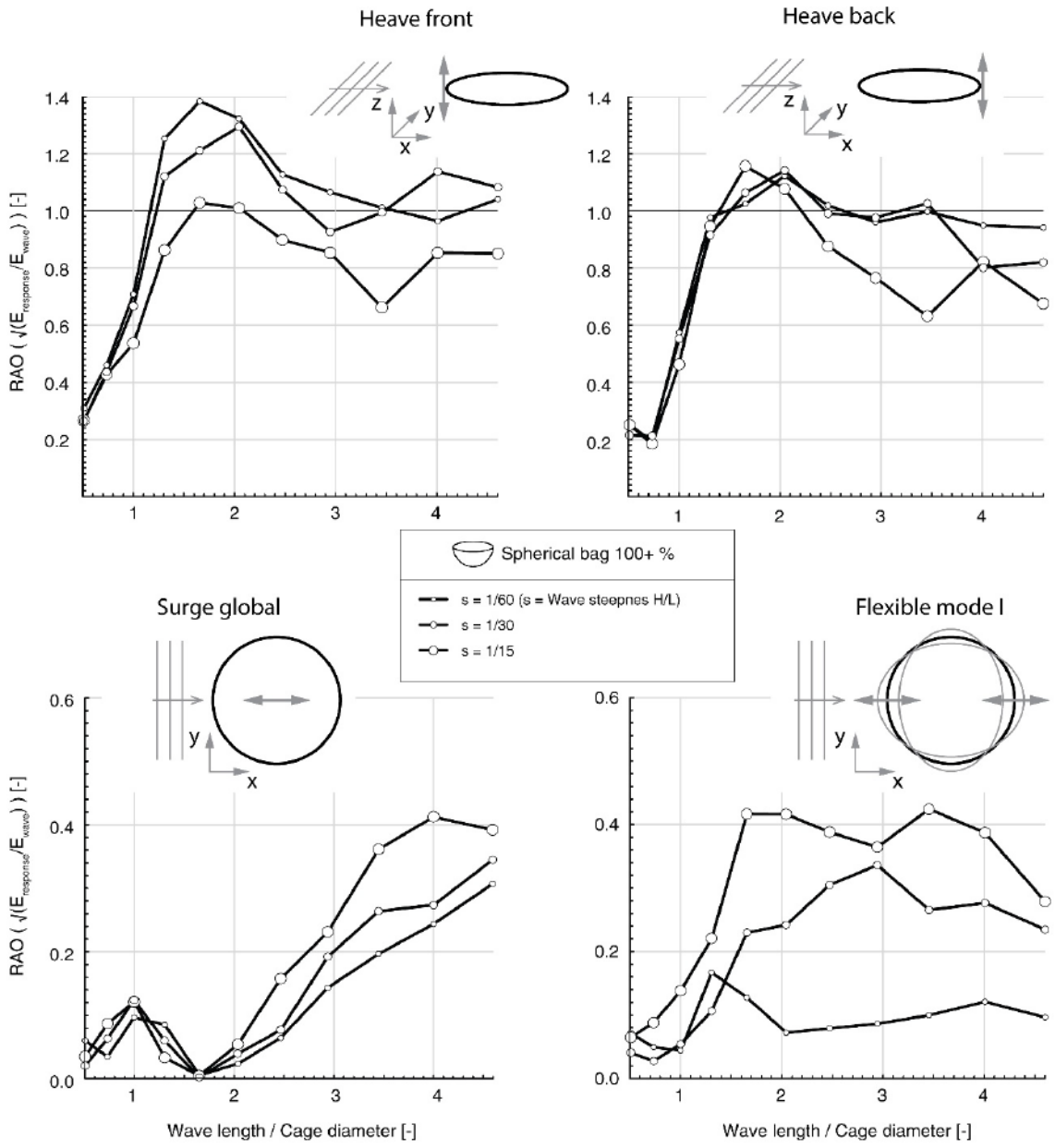

Figure 8. 1st harmonic response amplitude operator (RAO) for the spherical bag (dashed area in Figure 5). The calculation of RAO is explained in the caption of Figure 7.

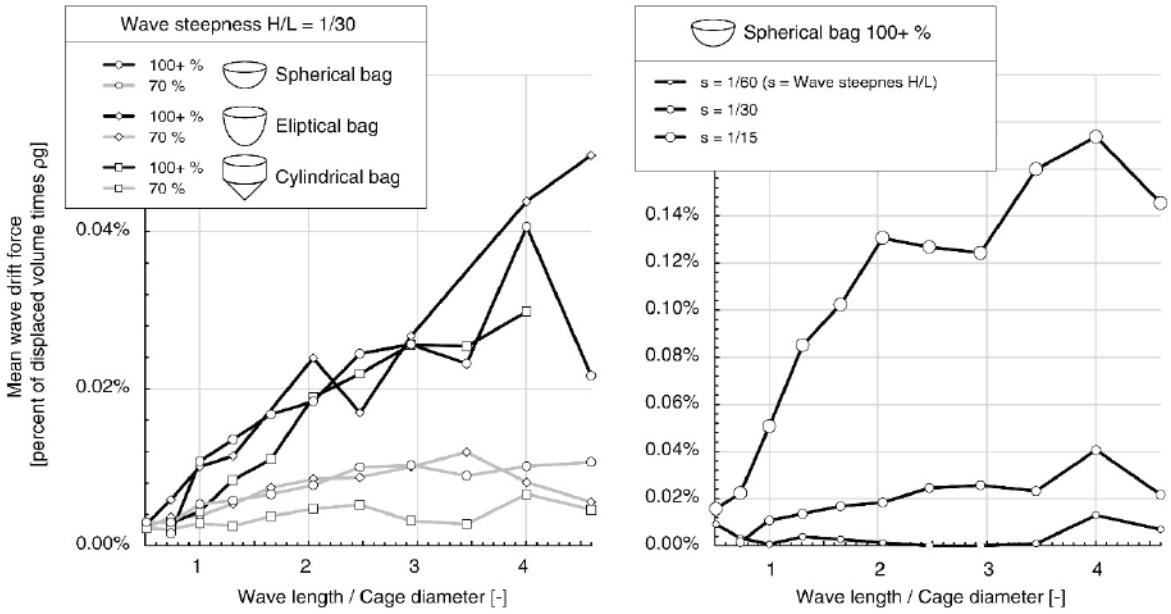

Figure 9. Mean wave drift force. The force is given as a percent of the displace volume (100%+ inflated state) times $\rho\, g$ (water density and the acceleration of gravity). The mean wave drift force is calculated from the mean surge displacement (x-direction) using the spring constant of the mooring lines along the x-axis. The contribution from the mooring along the y-axis to the force in x-direction is neglected. This is justified by the mean displacement in surge being less than 10 cm, and for such a displacement the force contribution from the y-direction mooring lines is less than 10% of the force in the x-direction mooring lines.